

Formulations of the extended boundary condition method for incident Gaussian beams using multiple-multipole expansions

A. DOICU and T. WRIEDT

Institut für Werkstofftechnik, Badgasteinerstrasse 3, 28359 Bremen, Germany

(Received 29 July 1996; revision received 15 November 1996)

Abstract. Novel formulations for improving the numerical stability of the extended boundary conditions method and extending its application to highly elongated dielectric objects illuminated by a Gaussian beam are described. The derived formulations are obtained as special cases of a general approach, which considers arbitrary complete system functions on the particle surface. The surface currents are approximated by multiple spherical expansions or, for a fixed azimuthal mode, by the lowest-order multipoles located inside the particle surface. Results illustrating the application of the procedures developed are presented.

1. Introduction

Electromagnetic scattering from non-spherical, perfectly conducting and homogeneous dielectric bodies using spherical vector wavefunctions (SVWFs) have been formulated in the form of the extended boundary condition method (EBCM) by Waterman [1].

Numerical difficulties of the standard, single-spherical-coordinate-based EBCM appear for scattering problems involving large aspect ratios. For such cases a large number of terms in the vector spherical harmonics expansion are required to describe the field variations. The matrix formulations include Hankel functions of large argument and orders which result in an ill-conditioned system of equations.

A number of modifications to this method have been suggested to ameliorate these problems. Numerical techniques such as the orthogonalization method [2] or the reinforced modified Gramm–Schmidt orthogonalization procedure [3] can be mentioned here. Bates and Wall [4] proposed the use of spheroidal wavefunctions for the expansion of the free-space Green dyadic and the choice of the form of the expansion for the induced surface currents, which is made in terms of functions natural to the surface of the scatterer. The spheroidal-coordinate-based EBCM [5] offers an aesthetically pleasing alternative, while other formal modifications of the EBCM were proposed by Boström [6].

The actual breakthrough enabling application to general geometries is to use multiple origins. This was apparently first proposed by Hafner [7] and independently by Ludwig [8], Eremin and Sveshnikov [9] and Leviatan *et al.* [10]. This technique is known as the generalized multipole technique (GMT) or discrete-sources method (DSM). Essentially, the unknown field in each domain is

approximated by several sets of functions with different origins. This representation of the solution satisfies the Maxwell equations and the unknown amplitudes are determined from the condition that the boundary values of the fields are close in a certain norm [11].

The iterative extended boundary condition method (IEBCM) is also based on the fact that an expansion using a single origin for objects with a large aspect ratio becomes numerically unstable [12, 13]. A first improvement is done by subdividing the interior of the object into several overlapping subregions and performing a spherical expansion for each. The continuity of the internal fields through the object is assured by enforcing the continuity of these expansions at several points in the overlapping regions. For applications involving relatively high-loss dielectric objects, an initial assumption of the surface fields is obtained by using the solution of the regular EBCM for a perfectly conducting object of the same shape while, for low-loss or lossless elongated particles, one used the Mie solution of a spherical object with the same dielectric properties. The original dielectric properties or the original geometry are built in gradually by reapplying EBCM through an iterative procedure.

In our paper we derive two formulations of the EBCM using multiple expansions with different origins. We expect to increase the stability of the method because multiple origins are more adequate to model the boundary geometry of a highly elongated particle.

2. Mathematical formulation

There are different possibilities to present the mathematical details of the EBCM. We note here that the Huygen principle used in this way has been variously known as the Schelkunoff equivalent current method, the Ewald–Osen extinction theorem or the null-field method [14]. It can be shown that the EBCM can be interpreted in terms of the method of moments introduced by Harrington [15]. In the method of moments, applied to the present problem, the unknown surface field can be expanded in terms of a large class of basis functions which may lead to different numerical properties of the solution. We present here a flexible scheme for surface currents determination by considering arbitrary complete system functions on the particle surface. This approach can be regarded as a general formulation of the EBCM.

Let us consider a three-dimensional space Ω , consisting of the union of a closed surface S , its interior Ω_i and its exterior Ω_s . We choose a point O within Ω_i to be the origin of a Cartesian coordinate system. An arbitrary point in Ω is denoted by Q , while an arbitrary point on S is denoted by M . Let $L_2(S_{\text{tan}})$ be the space of square integrable tangential vector functions on S .

The mathematical formulation of the scattering problem of an incident field $(\mathbf{E}_0, \mathbf{H}_0)$ by a homogeneous dielectric object with surface S is

$$\nabla \times \mathbf{E}_t = jk\mu_t \mathbf{H}_t, \quad \nabla \times \mathbf{H}_t = -jk\varepsilon_t \mathbf{E}_t \text{ in } \Omega_t, \quad (1)$$

where $t = s, i$, $\mathbf{n} \times (\mathbf{E}_0 + \mathbf{E}_s - \mathbf{E}_i) = \mathbf{0}$, $\mathbf{\bar{n}} \times (\mathbf{H}_0 + \mathbf{H}_s - \mathbf{H}_i) = \mathbf{0}$ on S and the radiation condition for $(\mathbf{E}_s, \mathbf{H}_s)$ is uniform over all possible radial directions. Here, \mathbf{n} is the outward unit normal to S , $k = \omega/c$, $\varepsilon_s, \mu_s > 0$, $\text{Im } \varepsilon_i, \mu_i \geq 0$ and $S \in C^{(2,a)}$. In this case there exists a unique solution for the boundary value problem (BVP) (1). In order to construct a solution close to the exact solution of the BVP (1) in

uniform metrics, it is sufficient to approximate the values of the incident field $(\mathbf{E}_0, \mathbf{H}_0)$ in the mean-square norm at the particle surface S [9, 11].

Let us consider the vector wavefunctions (not necessarily spherical) $\phi_{\hat{n}}^t(\mathbf{Q})$ and $\Psi_{\hat{n}}^t(\mathbf{Q})$, such as

$$\begin{aligned} \text{(I)} \quad & \nabla \times \phi_{\hat{n}}^t(\mathbf{Q}) = k_t \Psi_{\hat{n}}^t(\mathbf{Q}), \quad \nabla \times \Psi_{\hat{n}}^t(\mathbf{Q}) = k_t \phi_{\hat{n}}^t(\mathbf{Q}), \quad t = s, i, \\ \text{(II)} \quad & \phi_{\hat{n}}^i(\mathbf{Q}) \text{ and } \Psi_{\hat{n}}^i(\mathbf{Q}) \text{ are finite at the origin,} \\ \text{(III)} \quad & \phi_{\hat{n}}^s(\mathbf{Q}) \text{ and } \Psi_{\hat{n}}^s(\mathbf{Q}) \text{ satisfy the radiation condition.} \end{aligned} \quad (2)$$

Here, k_t is the wavenumber of the region Ω_t , that is $k_t = k(\varepsilon_t \mu_t)^{1/2}$.

Let us assume that the set of the tangential vector wavefunctions

$$\left\{ \left(\mathbf{n} \times \phi_{\hat{n}}^t(\mathbf{M}), -j \left(\frac{\varepsilon_t}{\mu_t} \right)^{1/2} (\mathbf{n} \times \Psi_{\hat{n}}^t(\mathbf{M})) \right); \right. \\ \left. \left(\mathbf{n} \times \Psi_{\hat{n}}^t(\mathbf{M}), -j \left(\frac{\varepsilon_t}{\mu_t} \right)^{1/2} (\mathbf{n} \times \phi_{\hat{n}}^t(\mathbf{M})) \right) \right\}; t = s, i; \hat{n} = 1, 2, \dots, \quad (3)$$

is complete on the surface S , that is for any field $(\mathbf{e}_0, \mathbf{h}_0)$ and any $\delta > 0$ there exists $\hat{N}_0 = \hat{N}_0(\delta)$ that for all $\hat{N} > \hat{N}_0$

$$\|\mathbf{e}_0 + \mathbf{e}_s^{\hat{N}} - \mathbf{e}_i^{\hat{N}}\| + \|\mathbf{h}_0 + \mathbf{h}_s^{\hat{N}} - \mathbf{h}_i^{\hat{N}}\| \leq \delta, \quad (4)$$

where

$$\begin{aligned} (\mathbf{e}_t^{\hat{N}}, \mathbf{h}_t^{\hat{N}}) = & \sum_{\hat{n}=1}^{\hat{N}} \alpha_{\hat{n}}^t \left(\mathbf{n} \times \phi_{\hat{n}}^t(\mathbf{M}), -j \left(\frac{\varepsilon_t}{\mu_t} \right)^{1/2} (\mathbf{n} \times \Psi_{\hat{n}}^t(\mathbf{M})) \right) \\ & + \beta_{\hat{n}}^t \left(\mathbf{n} \times \Psi_{\hat{n}}^t(\mathbf{M}), -j \left(\frac{\varepsilon_t}{\mu_t} \right)^{1/2} (\mathbf{n} \times \phi_{\hat{n}}^t(\mathbf{M})) \right), t = s, i. \end{aligned} \quad (5)$$

In equations (4) and (5) we find it convenient to use the short letter notations for the tangential components of the fields on S , that is $\mathbf{e}_t = \mathbf{n} \times \mathbf{E}_t(\mathbf{M})$, $\mathbf{h}_t = \mathbf{n} \times \mathbf{H}_t(\mathbf{M})$, where $t = s, i, 0$.

There are different schemes for determining the surface currents, for example the minimization of the defect functional in $L_2(S_{\text{tan}})$, or the point-matching method using overdetermined linear algebraic equations systems.

A possible scheme for determination of the surface currents can be constructed in the following form. Let us consider the complete system functions

$$\left\{ \left(\mathbf{n} \times \mathbf{n} \times \phi_{\hat{n}}^t(\mathbf{M}), j \left(\frac{\mu_t}{\varepsilon_t} \right)^{1/2} (\mathbf{n} \times \mathbf{n} \times \Psi_{\hat{n}}^t(\mathbf{M})) \right); \right. \\ \left. \left(\mathbf{n} \times \mathbf{n} \times \Psi_{\hat{n}}^t(\mathbf{M}), j \left(\frac{\mu_t}{\varepsilon_t} \right)^{1/2} (\mathbf{n} \times \mathbf{n} \times \phi_{\hat{n}}^t(\mathbf{M})) \right) \right\}; t = s, i; \hat{n} = 1, 2, \dots, \quad (6)$$

on S and write the boundary conditions

$$\mathbf{e}_0 + \mathbf{e}_s - \mathbf{e}_i = 0, \quad \mathbf{h}_0 + \mathbf{h}_s - \mathbf{h}_i = 0$$

in an integral form

$$\int_S \delta \mathbf{e} \cdot \boldsymbol{\phi}_{\hat{\mathbf{n}}}^{\dagger}(\mathbf{M}) + j \left(\frac{\mu_t}{\varepsilon_t} \right)^{1/2} \delta \mathbf{h} \cdot \boldsymbol{\Psi}_{\hat{\mathbf{n}}}^{\dagger}(\mathbf{M}) = 0, \quad (7)$$

$$\int_S \delta \mathbf{e} \cdot \boldsymbol{\Psi}_{\hat{\mathbf{n}}}^{\dagger}(\mathbf{M}) + j \left(\frac{\mu_t}{\varepsilon_t} \right)^{1/2} \delta \mathbf{h} \cdot \boldsymbol{\phi}_{\hat{\mathbf{n}}}^{\dagger}(\mathbf{M}) = 0 \quad t = s, i; i = 1, 2, \dots,$$

where $\delta \mathbf{e} = \mathbf{e}_0 + \mathbf{e}_s - \mathbf{e}_i$ and $\delta \mathbf{h} = \mathbf{h}_0 + \mathbf{h}_s - \mathbf{h}_i$. The set (7) can be regarded as the 'extended integral equations' of the surface currents. The amplitudes of the approximate surface currents $(\mathbf{e}_i^{\hat{N}}, \mathbf{h}_i^{\hat{N}})$ are obtained by substituting $(\mathbf{e}_0 + \mathbf{e}_s^{\hat{N}} - \mathbf{e}_i^{\hat{N}}, \mathbf{h}_0 + \mathbf{h}_s^{\hat{N}} - \mathbf{h}_i^{\hat{N}})$ in equations (7) and considering the first $4\hat{N}$ integral equations (7).

In contrast with the minimization method, which leads to a normal system of equations and can be regarded as a Galerkin method for the unitary operator, the above procedure can be considered as a non-Galerkin moment method, because the testing tangential vector functions are obtained from the basis functions by a rotation of 90° about the unit normal. The main advantage of this choice consists of the decoupling of the surface currents problem into two independent sub-problems for the tangential components of the internal and the scattered field respectively. This decoupling follows from the Green formula applied to the vector wave functions $\boldsymbol{\phi}_{\hat{\mathbf{n}}}^{\dagger}(\mathbf{Q})$ and $\boldsymbol{\Psi}_{\hat{\mathbf{n}}}^{\dagger}(\mathbf{Q})$. It is simple to show that, if the sequences $(\mathbf{e}_i^{\hat{N}}, \mathbf{h}_i^{\hat{N}})$ and $(\mathbf{e}_s^{\hat{N}}, \mathbf{h}_s^{\hat{N}})$, as solutions of two separate problems (7), converge in the mean-square norm on S at $(\mathbf{e}_i, \mathbf{h}_i)$ and $(\mathbf{e}_s, \mathbf{h}_s)$, respectively, then $(\mathbf{e}_i, \mathbf{h}_i)$ and $(\mathbf{e}_s, \mathbf{h}_s)$ are the tangential components of the unique solution of BVP (1). Furthermore, an estimate for the *a posteriori* error can be given by computing the discrepancy of the residual tangential fields on the surface of the scatterer.

In view of the EBCM, one considers only the independent subproblem for the internal surface currents $(\mathbf{e}_i^{\hat{N}}, \mathbf{h}_i^{\hat{N}})$ and computes the scattered field by using the Huygens principle. Thus a general scheme for computing the amplitudes of the internal surface currents $(\mathbf{e}_i^{\hat{N}}, \mathbf{h}_i^{\hat{N}})$ consists of a set of $2\hat{N}$ integral equations

$$\int_S (\mathbf{e}_i^{\hat{N}} - \mathbf{e}_0) \cdot \boldsymbol{\phi}_{\hat{\mathbf{n}}}^{\dagger}(\mathbf{M}) + j \left(\frac{\mu_s}{\varepsilon_s} \right)^{1/2} (\mathbf{h}_i^{\hat{N}} - \mathbf{h}_0) \cdot \boldsymbol{\Psi}_{\hat{\mathbf{n}}}^{\dagger}(\mathbf{M}) = 0, \quad (8)$$

$$\int_S (\mathbf{e}_i^{\hat{N}} - \mathbf{e}_0) \cdot \boldsymbol{\Psi}_{\hat{\mathbf{n}}}^{\dagger}(\mathbf{M}) + j \left(\frac{\mu_s}{\varepsilon_s} \right)^{1/2} (\mathbf{h}_i^{\hat{N}} - \mathbf{h}_0) \cdot \boldsymbol{\phi}_{\hat{\mathbf{n}}}^{\dagger}(\mathbf{M}) = 0, \hat{n} = 1, \dots, \hat{N}$$

which reduces to a linear algebraic system by considering for $(\mathbf{e}_i^{\hat{N}}, \mathbf{h}_i^{\hat{N}})$ the representation given in equation (5).

Once the internal surface currents are determined, the approximate solution of the scattered field is obtained by using the integral representation

$$\mathbf{E}_s^{\hat{N}}(\mathbf{Q}) = \nabla \times \int_S \mathbf{e}_i^{\hat{N}} \cdot \mathbf{G}(k_s, \mathbf{M}, \mathbf{Q}) dS - \nabla \times \nabla$$

$$\times \int_S \frac{1}{jk\varepsilon_s} \mathbf{h}_i^{\hat{N}} \cdot \mathbf{G}(k_s, \mathbf{M}, \mathbf{Q}) dS, \mathbf{Q} \in \Omega_s, \quad (9)$$

where $G(k_s, \mathbf{M}, \mathbf{Q})$ is the free-space transverse dyadic Green function. We note here that our presentation concentrates on the question of obtaining an approximate solution on the surface S . In the T -matrix scheme, one furthermore expands the scattered field outside a circumscribed sphere in terms of SVWFs, truncates

this expansion at the index \hat{N} and computes the transition matrix which relates the scattered field coefficients to the incident field coefficients. Essentially, once the internal surface currents are determined a formal solution of the scattered field can be constructed in the form (9)

The far-field vector amplitude $\mathbf{F}_s^{\hat{N}}(\theta_Q, \varphi_Q)$ of the scattered field is calculated from

$$\lim_{r_Q \rightarrow \infty} [\mathbf{E}_s^{\hat{N}}(\mathbf{Q})] = \mathbf{F}_s^{\hat{N}}(\theta_Q, \varphi_Q) \frac{\exp(jk_s r_Q)}{r_Q} \quad (10)$$

and the differential scattering cross-section from

$$\sigma_d^{\hat{N}} = |\mathbf{F}_s^{\hat{N}}|^2. \quad (11)$$

Here $(r_Q, \theta_Q, \varphi_Q)$ are the spherical coordinates of the point Q.

A similar version can be constructed if one considers the subproblem for the tangential components of the scattered field $(\mathbf{e}_s^{\hat{N}}, \mathbf{h}_s^{\hat{N}})$. In this case, one replaces $\mathbf{e}_i^{\hat{N}} - \mathbf{e}_0$ and $\mathbf{h}_i^{\hat{N}} - \mathbf{h}_0$ in equation (8) by $\mathbf{e}_s^{\hat{N}} + \mathbf{e}_0$ and $\mathbf{h}_s^{\hat{N}} + \mathbf{h}_0$ respectively, and the index i by s and reciprocally. We note here that the independent exterior subproblem for the surface currents, in terms of SVWFs with a single origin, was also obtained by Hizel [16] starting from the vector potential formulation

For our next presentation, we write equation (8) in short-hand form as

$$\begin{aligned} a(\mathbf{e}_i^{\hat{N}} - \mathbf{e}_0, \mathbf{h}_i^{\hat{N}} - \mathbf{h}_0, \phi_{\hat{n}}^{\hat{N}}(\mathbf{M}), \psi_{\hat{n}}^{\hat{N}}(\mathbf{M})) &= 0 \\ b(\mathbf{e}_i^{\hat{N}} - \mathbf{e}_0, \mathbf{h}_i^{\hat{N}} - \mathbf{h}_0, \phi_{\hat{n}}^{\hat{N}}(\mathbf{M}), \psi_{\hat{n}}^{\hat{N}}(\mathbf{M})) &= 0 \quad \hat{n} = 1, \dots, \hat{N}, \end{aligned} \quad (12)$$

where the functional a designates the first integral equation and b the second integral equation.

Effective schemes for determination of surface currents can be obtained by considering different complete system functions in $L_2(S_{\text{tan}})$. In the present paper we restrict our analysis to complete system functions derived from SVWFs, that is

$$\begin{aligned} \mathbf{M}_{mn}^{1,3}(k\mathbf{r}_Q) &= z_n(kr_Q) \left(jm \frac{P_n^{|m|}(\cos \theta)}{\sin \theta} \mathbf{i}_\theta - \frac{dP_n^{|m|}(\cos \theta)}{d\theta} \mathbf{i}_\varphi \right) \exp(jm\varphi), \\ \mathbf{N}_{mn}^{1,3}(k\mathbf{r}_Q) &= \left[n(n+1) \frac{z_n(kr_Q)}{kr_Q} P_n^{|m|}(\cos \theta) \mathbf{i}_r \right. \\ &\quad \left. + \frac{[kr_Q z_n(kr_Q)]'}{kr_Q} \left(\frac{dP_n^{|m|}(\cos \theta)}{d\theta} \mathbf{i}_\theta + jm \frac{P_n^{|m|}(\cos \theta)}{\sin \theta} \mathbf{i}_\varphi \right) \right] \exp(jm\varphi), \end{aligned} \quad (13)$$

where (r_Q, θ, φ) are the spherical coordinates of the observation point Q, $(\mathbf{i}_r, \mathbf{i}_\theta, \mathbf{i}_\varphi)$ are the unit vectors in spherical coordinates, $z_n(kr_Q)$ designates the spherical Bessel functions $j_n(kr_Q)$ or the spherical Hankel functions $h_n^1(kr_Q)$, and $P_n^m(\cos \theta)$ denotes the associated Legendre polynomial of order n , m .

We have the following results.

(A) The set of the tangential components of the regular and radiating SVWFs, given by equations (3) and (6) with $\phi_{\hat{n}}^{\hat{N}}(\mathbf{Q}) = \mathbf{M}_{mn}^{3,1}(k_{s,i} \mathbf{r}_Q)$, $\psi_{\hat{n}}^{\hat{N}}(\mathbf{Q}) = \mathbf{N}_{mn}^{3,1}(k_{s,i} \mathbf{r}_Q)$, where $m \in \mathbb{Z}$ and $n \geq \max(1, |m|)$, is complete on S . Here \hat{n} is an index incorporating m and n . The completeness of the above system has been discussed by Müller [17], Aydin and Hizal [18] and

also originally by Waterman [1]. We note, however, that the completeness of equation (6) follows directly from the uniqueness of the coupled null-field integral equation for the electric and magnetic surface currents, which are considered as independent unknowns [19].

- (B) Let us consider a rigid translation \mathbf{r}_p of the original coordinate system and denote by O_p the origin of the new coordinate system, so that $\mathbf{r}_{pQ} = \mathbf{r}_Q - \mathbf{r}_p$. Then the system of the tangential components of the SVWFs with a shifted origin, given by equations (3) and (6) with $\phi_{\hat{h}}^{s,i}(\mathbf{Q}) = \mathbf{M}_{mm}^{3,1}(k_{s,i}\mathbf{r}_{pQ})$, $\psi_{\hat{h}}^{s,i}(\mathbf{Q}) = \mathbf{N}_{mm}^{3,1}(k_{s,i}\mathbf{r}_{pQ})$, where $m \in \mathbb{Z}$ and $n \geq \max(1, |m|)$, is complete on S .
- (C) Let us consider a set of poles $\{z_n\}_{n=1}^{\infty}$ located on the z axis with Ω_i . Let the set $\{z_n\}_{n=1}^{\infty}$ have at least one limit point in Ω_i ; then the tangential components of the lowest-order SVWF given by equations (3) and (6) with $\phi_{\hat{h}}^{s,i}(\mathbf{Q}) = \mathbf{M}_{m,|m|+1}^{3,1}(k_{s,i}\mathbf{r}_{nQ})$, $\psi_{\hat{h}}^{s,i}(\mathbf{Q}) = \mathbf{N}_{m,|m|+1}^{3,1}(k_{s,i}\mathbf{r}_{nQ})$, where $m \in \mathbb{Z}$ and $n \geq 1$ and $l = 1$ if $m = 0$ and $l = 0$ otherwise, is complete on S . The completeness of this set can be demonstrated using the completeness of the tangential vector wavefunctions referenced to a single origin and an integral representation for the coefficients of the vector addition theorem for SVWFs under a translation of the coordinate origin. We note here that a similar complete system of functions was introduced by Eremin and Sveshnikov [9] and Eremin *et al.* [11] by considering the electric and magnetic Hertz vectors constructed in a Cartesian basis using the lowest-order multipoles for the scalar wave equation. Other non-spherical complete system functions were obtained by Kersten [20].

Corresponding to the above complete system functions, the following schemes for surface currents determination can be considered.

The amplitudes of the approximate solution of the internal surface currents $(\mathbf{e}_i^{\hat{N}}, \mathbf{h}_i^{\hat{N}})$, written in the following explicit forms.

- (A) For a single origin, we have

$$\begin{aligned} (\mathbf{e}_i^{\hat{N}}, \mathbf{h}_i^{\hat{N}}) = & \sum_{m=-M}^M \sum_{n \geq \max(1, |m|)}^N \alpha_{mn}^i \left(\mathbf{n} \times \mathbf{M}_{mn}^1(k_i \mathbf{r}_M), -j \left(\frac{\varepsilon_i}{\mu_i} \right)^{1/2} (\mathbf{n} \times \mathbf{N}_{mn}^1(k_i \mathbf{r}_M)) \right) \\ & + \beta_{mn}^i \left(\mathbf{n} \times \mathbf{N}_{mn}^1(k_i \mathbf{r}_M), -j \left(\frac{\varepsilon_i}{\mu_i} \right)^{1/2} (\mathbf{n} \times \mathbf{M}_{mn}^1(k_i \mathbf{r}_M)) \right). \end{aligned} \quad (14)$$

- (B) For a finite collection of poles $\{\mathbf{r}_p\}_{p=1}^{N_p}$, as

$$\begin{aligned} (\mathbf{e}_i^{\hat{N}}, \mathbf{h}_i^{\hat{N}}) = & \sum_{p=1}^{N_p} \sum_{m=-M(p)}^{M(p)} \sum_{n \geq \max(1, |m|)}^{M(p)} \alpha_{mn}^{i(p)} \\ & \times \left(\mathbf{n} \times \mathbf{M}_{mn}^1(k_i \mathbf{r}_{pM}), -j \left(\frac{\varepsilon_i}{\mu_i} \right)^{1/2} (\mathbf{n} \times \mathbf{N}_{mn}^1(k_i \mathbf{r}_{pM})) \right) \\ & + \beta_{mn}^{i(p)} \left(\mathbf{n} \times \mathbf{N}_{mn}^1(k_i \mathbf{r}_{pM}), -j \left(\frac{\varepsilon_i}{\mu_i} \right)^{1/2} (\mathbf{n} \times \mathbf{M}_{mn}^1(k_i \mathbf{r}_{pM})) \right). \end{aligned} \quad (15)$$

(C) For a set of poles $\{\zeta_n\}_{n=1}^N$, having at least one limit point in Ω_i , as

$$\begin{aligned}
 (\mathbf{e}_i^{\hat{N}}, \mathbf{h}_i^{\hat{N}}) &= \sum_{m=-M}^M \sum_{n \geq 1}^N \\
 &\times \alpha_{mn}^i \left(\mathbf{n} \times \mathbf{M}_{m,|m|+l}^1(k_i \mathbf{r}_{nM}), -j \left(\frac{\varepsilon_i}{\mu_i} \right)^{1/2} (\mathbf{n} \times \mathbf{N}_{m,|m|+l}^1(k_i \mathbf{r}_{nM})) \right) \\
 &+ \beta_{mn}^i \left(\mathbf{n} \times \mathbf{N}_{m,|m|+l}^1(k_i \mathbf{r}_{nM}), -j \left(\frac{\varepsilon_i}{\mu_i} \right)^{1/2} (\mathbf{n} \times \mathbf{M}_{m,|m|+l}^1(k_i \mathbf{r}_{nM})) \right) \\
 & \quad l = 1 \text{ if } m = 0 \text{ and } l = 0 \text{ otherwise.} \quad (16)
 \end{aligned}$$

These are obtained as a solution of the following truncated system of integral equations:

$$\begin{aligned}
 (A) \quad a(\mathbf{e}_i^{\hat{N}} - \mathbf{e}_0, \mathbf{h}_i^{\hat{N}} - \mathbf{h}_0, \mathbf{M}_{mn}^3(k_s \mathbf{r}_M), \mathbf{N}_{mn}^3(k_s \mathbf{r}_M)) &= 0, \\
 b(\mathbf{e}_i^{\hat{N}} - \mathbf{e}_0, \mathbf{h}_i^{\hat{N}} - \mathbf{h}_0, \mathbf{M}_{mn}^3(k_s \mathbf{r}_M), \mathbf{N}_{mn}^3(k_s \mathbf{r}_M)) &= 0, \quad (17) \\
 m = -M, \dots, M, n = \max(1, |m|), \dots, N,
 \end{aligned}$$

$$\begin{aligned}
 (B) \quad a(\mathbf{e}_i^{\hat{N}} - \mathbf{e}_0, \mathbf{h}_i^{\hat{N}} - \mathbf{h}_0, \mathbf{M}_{mp}^3(k_s \mathbf{r}_{pM}), \mathbf{N}_{mp}^3(k_s \mathbf{r}_{pM})) &= 0, \\
 b(\mathbf{e}_i^{\hat{N}} - \mathbf{e}_0, \mathbf{h}_i^{\hat{N}} - \mathbf{h}_0, \mathbf{M}_{mp}^3(k_s \mathbf{r}_{pM}), \mathbf{N}_{mp}^3(k_s \mathbf{r}_{pM})) &= 0, \quad (18) \\
 p = 1, \dots, N_p, m = -M(p), \dots, M(p), n = \max(1, |m|), \dots, N(p),
 \end{aligned}$$

$$\begin{aligned}
 (C) \quad a(\mathbf{e}_i^{\hat{N}} - \mathbf{e}_0, \mathbf{h}_i^{\hat{N}} - \mathbf{h}_0, \mathbf{M}_{m,|m|+l}^3(k_s \mathbf{r}_{nM}), \mathbf{N}_{m,|m|+l}^3(k_s \mathbf{r}_{nM})) &= 0, \\
 b(\mathbf{e}_i^{\hat{N}} - \mathbf{e}_0, \mathbf{h}_i^{\hat{N}} - \mathbf{h}_0, \mathbf{M}_{m,|m|+l}^3(k_s \mathbf{r}_{nM}), \mathbf{N}_{m,|m|+l}^3(k_s \mathbf{r}_{nM})) &= 0, \quad (19) \\
 m = -M, \dots, M, n = 1, \dots, N, l = 1 \text{ if } m = 0 \text{ and } l = 0 \text{ otherwise.}
 \end{aligned}$$

Form (A) essentially represents the classical version of the EBCM introduced by Waterman. One recognizes the functions a and b as the expansion coefficients of the total electric field in terms of SVWFs. In this case, the set (17) represents the null-field condition for the exterior field within an inscribed sphere with centre O .

Form (B) is appropriate to the GMT. The surface currents are approximated in the mean-square norm by normal multipole expansions with different origins, and the null-field condition for the exterior field is simultaneously imposed in different inscribed spheres. The main difference consists of the fact that this method is a combination of the duality of entire-domain bases for exterior fields and multiple-domain bases for interior fields. We note here that the locations of the spheres where the null-field condition is imposed may be different from the positions of the poles where the internal field approximation is considered.

Form (C) represents a modified version of the EBCM where the surface currents are approximated, for a fixed value of the azimuthal mode m , by the

lowest-order multipoles located on the z axis. Again, the positions of the poles in equations (16) and (19) may be different.

For a body of revolution the choice of multipoles situated on the symmetry axis of the particle makes it possible to reduce the problem of surface approximation of current distributions to a sequence of one-dimensional problems relative to Fourier harmonics of the surface currents.

We call, by convention, the second and the third formulations the multiple-multipole extended boundary condition methods (MMEBCMs).

3. Numerical results

Using the analytical development provided in section 2, we present comparisons of numerical computations for the verifications of the inherent accuracy of the proposed techniques. The differential scattering patterns are given for a series of test problems and compared with those obtained by the use of the classical version of the EBCM or otherwise available results.

Our computer code is for axisymmetrical particles illuminated by a Gaussian beam. The scattering geometry is shown in figure 1. We define the original beam coordinate system $OXYZ$ so that the centre of the Gaussian beam waist is located at the point O . The waist radius of the Gaussian beam is w_0 and the direction of propagation is along the Z axis. The polarization direction of the incident electric field and the X axis enclose an angle α_{pol} . The centre of the scatterer is located at the point o of a Cartesian coordinate system $oxyz$, which is called by convention the *particle location system*. The particle is oriented with the symmetry axis in

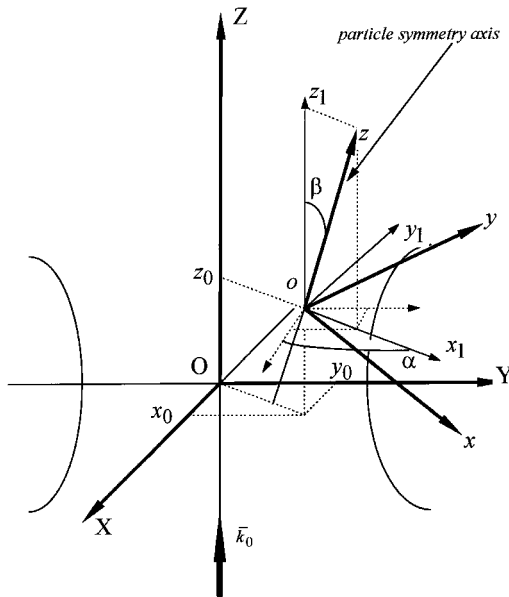


Figure 1. Scattering geometry showing the beam coordinate system $OXYZ$ and the particle location system $oxyz$. The direction of incidence is Z , and the symmetry axis of the object is z and is oriented at angles (α, β) . The coordinates of the particle centre in the beam frame are (x_0, y_0, z_0) .

the (α, β) direction referenced to the beam coordinate system. We denote by (x_0, y_0, z_0) the coordinates of the particle centre in the beam frame.

There are different possibilities for implementing a Gaussian beam description in the proposed forms of the EBCM. One of these techniques considers the analytic fifth-order beam description of Barton *et al.* [21] for \mathbf{e}_0 and \mathbf{h}_0 . In this case the integration over the particle surface in equation (8) must be numerically performed. Another method consists of using the partial waves decomposition of Gaussian beams. One recognizes the general form of the functionals a and b in equations (17)–(19) as the expansion coefficients, in terms of regular SVWFs, of the incident Gaussian beam, written in a translated coordinate system $o_p x_p y_p z_p$:

$$\begin{aligned} a(\mathbf{e}_0, \mathbf{h}_0, \mathbf{M}_{mn}^3(k_s \mathbf{r}_{pM}), \mathbf{N}_{mn}^3(k_s \mathbf{r}_{pM})) &= \frac{j\pi}{k_s^2} E_0 \varepsilon_s^{1/2} a_{-mn}^{(p)}, \\ b(\mathbf{e}_0, \mathbf{h}_0, \mathbf{M}_{mn}^3(k_s \mathbf{r}_{pM}), \mathbf{N}_{mn}^3(k_s \mathbf{r}_{pM})) &= \frac{j\pi}{k_s^2} E_0 \varepsilon_s^{1/2} a_{-mn}^{(p)}. \end{aligned} \quad (20)$$

The system $o_p x_p y_p z_p$ is obtained by a rigid translation of the particle coordinate system $oxyz$ with z_p along the z axis. The coordinates of the new origin o_p are given by

$$x_0^{(p)} = x_0 + z_p \sin \beta \cos \alpha, \quad y_0^{(p)} = y_0 + z_p \sin \beta \sin \alpha, \quad z_0^{(p)} = z_0 + z_p \cos \beta. \quad (21)$$

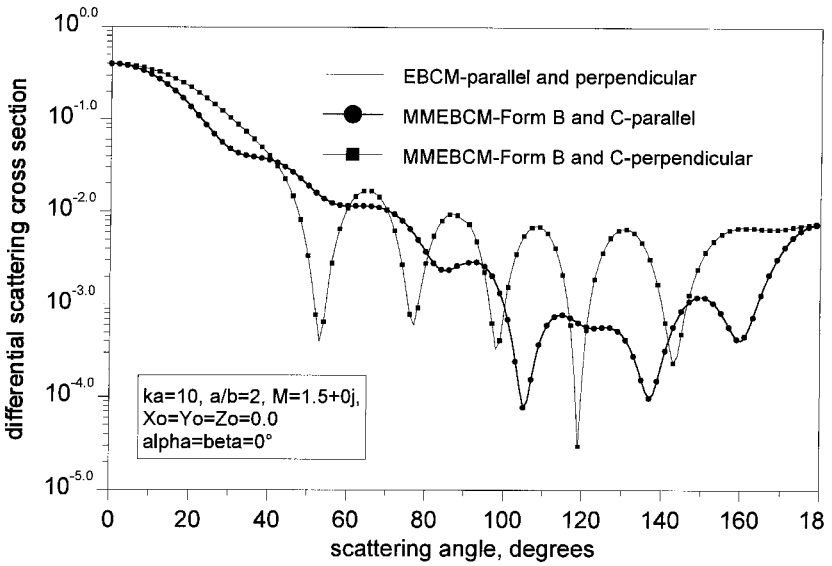
The expansion coefficients, or the beam shape coefficients, are computed by using the generalized localized approximation and the addition theorem for SVWFs under coordinate rotations [22];

$$\begin{aligned} \begin{pmatrix} a_{mn}^{(p)} \\ b_{mn}^{(p)} \end{pmatrix} &= \sum_{m'=-n}^n R_{m'n}^{mm'}(\alpha - \alpha_{\text{pol}}, \beta, 0) \begin{pmatrix} a_{m'n}^{(p)} \\ b_{m'n}^{(p)} \end{pmatrix}, \\ \begin{pmatrix} a_{m'n}^{(p)} \\ b_{m'n}^{(p)} \end{pmatrix} &= (-1)^{m'-1} C_{m'n} K_{m'n} \bar{P}_0^0 \exp(jk_s z_0^{(p)}) \\ &\times \frac{1}{2} \left[\exp[j(m'-1)\varphi_0] J_{m'-1} \left(2 \frac{\bar{Q} \rho_0 \rho_n}{w_0^2} \right) \right. \\ &\left. \pm \exp[j(m'+1)\varphi_0] J_{m'+1} \left(2 \frac{\bar{Q} \rho_0 \rho_n}{w_0^2} \right) \right], \end{aligned} \quad (22)$$

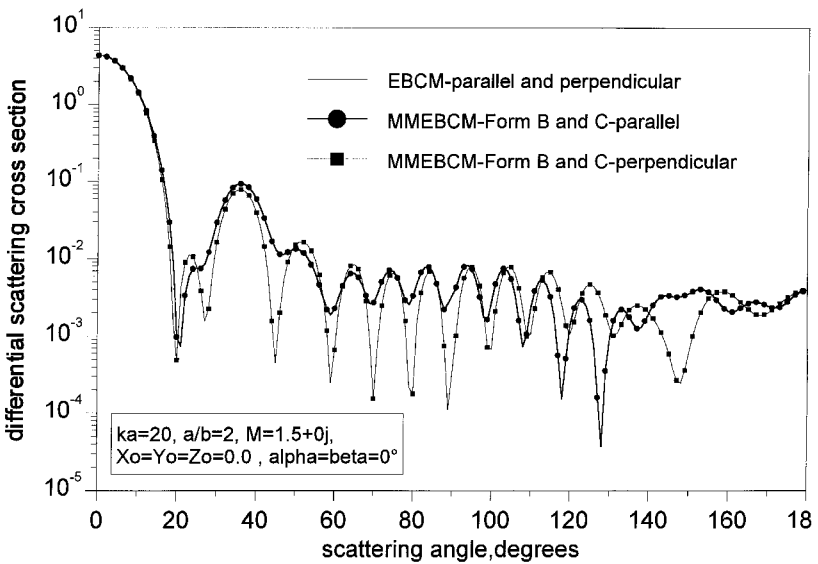
where $C_{m'n} = 4j^{n-1} (n + |m'|)! / (n - |m'|)!$ is a normalization constant,

$$K_{m'n} = \begin{cases} (-j)^{|m'|} \frac{j}{(n + 0.5)^{|m'|+1}}, & m' \neq 0, \\ \frac{n(n+1)}{n+0.5}, & m' = 0, \end{cases}$$

is a correction factor and



(a)

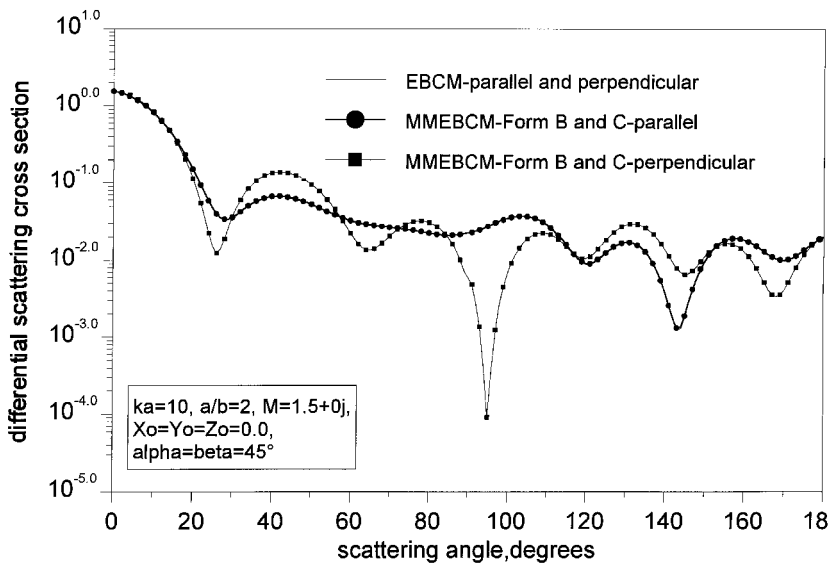


(b)

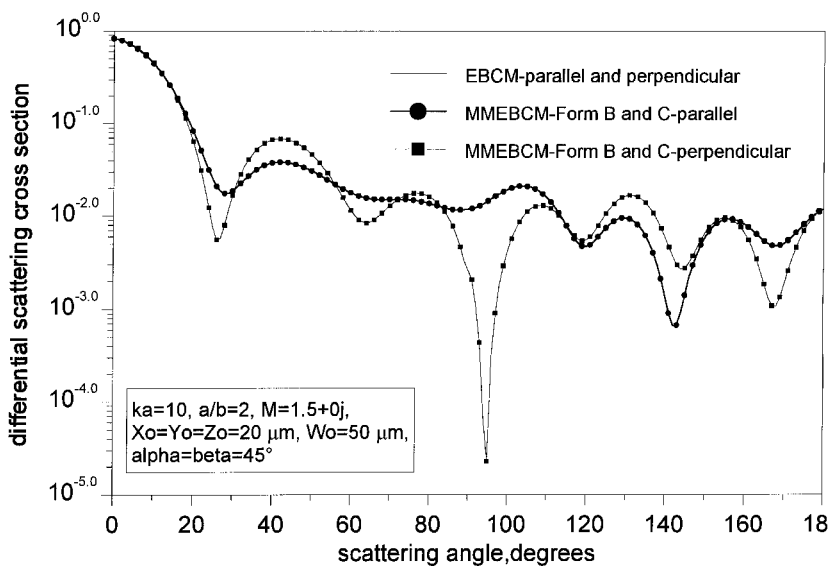
Figure 2. Plots of the normalized DSCS patterns for spheroidal particles with $M = 1.5$, $a/b = 2$: (a) $ka = 10$; (b) $ka = 20$. The position of the particles is $x_0 = y_0 = z_0 = 0$ and the orientation is $\alpha = \beta = 0^\circ$.

$$\bar{\Psi}_0^0 = j\bar{Q} \cdot \exp\left(\frac{-j\bar{Q}\rho_0^2}{w_0^2}\right) \cdot \exp\left(\frac{-j\bar{Q}(n+0.5)^2}{k_s^2 w_0^2}\right)$$

$$\rho_n = \frac{n+0.5}{k_s}, \bar{Q} = \frac{1}{(j - 2z_0^{(p)}/l)}, \rho_0 = [(x_0^{(p)})^2 + (y_0^{(p)})^2]^{1/2}, \varphi_0 = \tan^{-1}\left(\frac{x_0^{(p)}}{y_0^{(p)}}\right).$$



(a)



(b)

Figure 3. Plots of the normalized DSCS patterns for spheroidal particles of $M = 1.5$, $a/b = 2$, $ka = 10$, having a position and an orientation given by (a) $x_0 = y_0 = z_0 = 0$, $\alpha = \beta = 45^\circ$, and (b) $x_0 = y_0 = z_0 = 20 \mu\text{m}$, $\alpha = \beta = 45^\circ$.

Here, $R_{m'n}^{mm}(\alpha, \beta, \gamma)$ is the rotation matrix of the Euler angles (α, β, γ) which transforms the SVWFs under successive rotations of the coordinate system.

Our first objective is to demonstrate the validity of our EBCM formulations based on multiple-multipole expansions using for comparison the standard formulation of the EBCM as a reference. We shall be concerned with the scattering

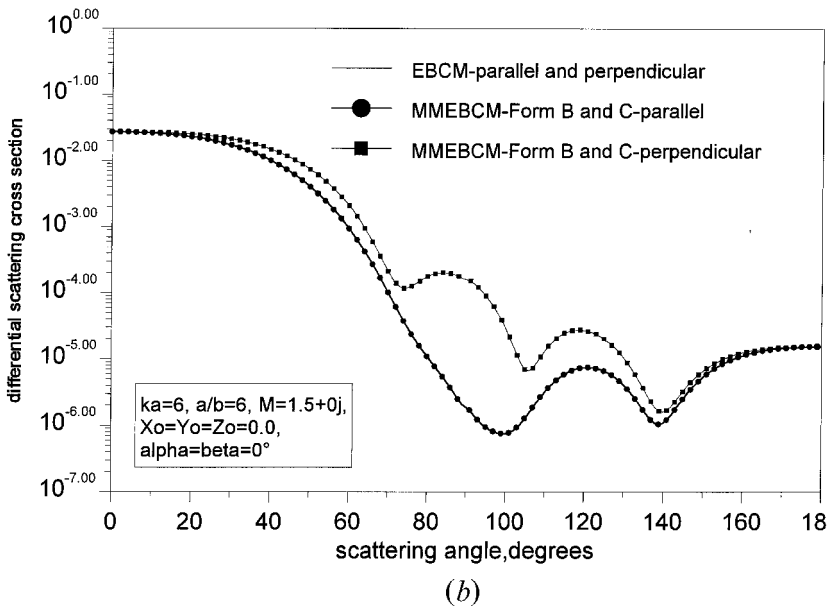
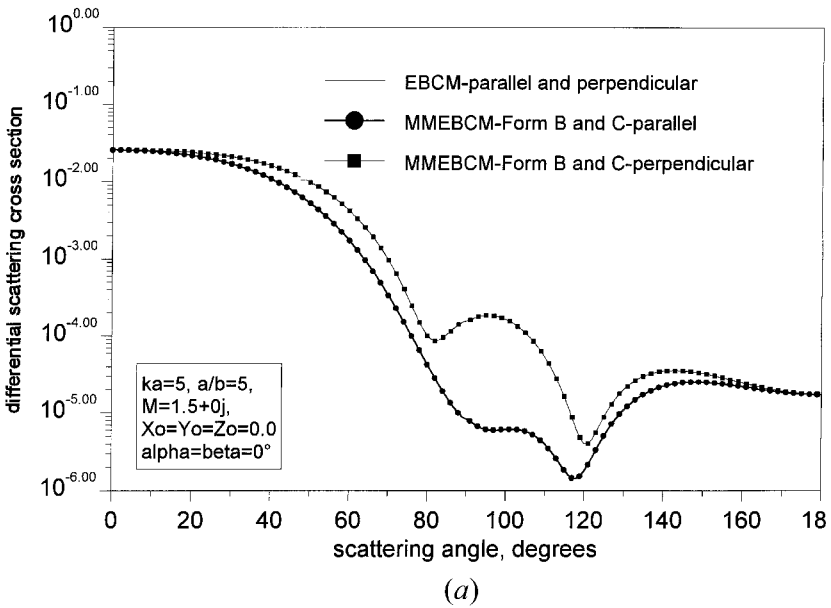


Figure 4. Plots of the normalized DSCS patterns for spheroidal particles with $M = 1.5$: (a) $a/b = 5$, $ka = 5$; (b) $a/b = 6$, $ka = 6$. The position of the particles is $x_0 = y_0 = z_0 = 0$ and the orientation is $\alpha = \beta = 0^\circ$.

by spheroidal lossless dielectric objects with a refractive index $M = 1.5$. Specifically, the differential scattering cross-section (DSCS), normalized by πa^2 , where a is the length of the semimajor axis, will be evaluated for prolate spheroids. Scatterers with different size parameters and eccentricities, having arbitrary positions and orientations in the Gaussian beam, are considered. The incident

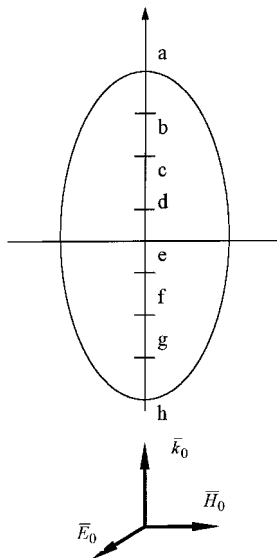
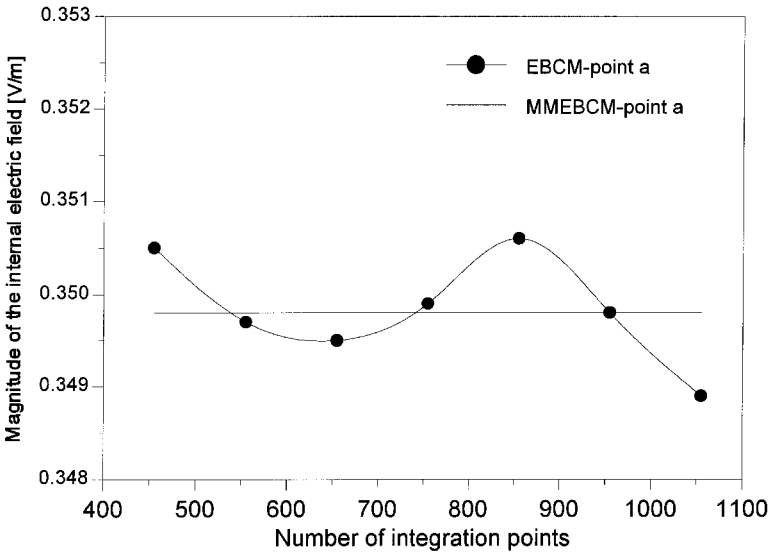


Figure 5. Illustration of the geometric locations of points used in the evaluation of the internal fields.

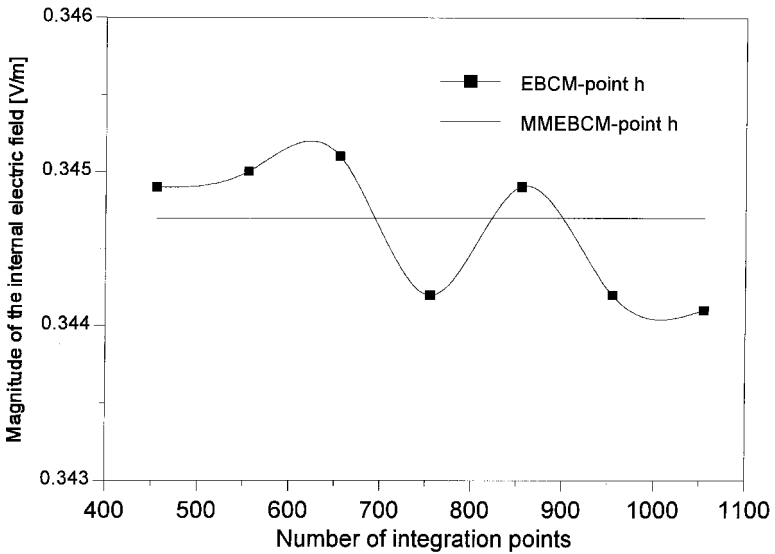
Table 1. Comparison of the magnitude of the internal electric-field distribution at selected equidistant points along the symmetry axis with the EBCM and the MMEBCM. The case of an spheroidal particle with $M = 2.236$, $a/b = 4$ and $ka = 1.35$ is considered.

Location of field points	Internal electric field (V m^{-1})	
	EBCM	MMEBCM, forms (B) and (C)
a	0.3816	0.3817
b	0.4062	0.4062
c	0.4216	0.4216
d	0.4261	0.4261
e	0.4202	0.4202
f	0.4065	0.4065
g	0.3876	0.3876
h	0.3654	0.3655

wave is linearly polarized and the polarization direction encloses an angle of 45° with the X axis. The scattered field will be evaluated over the azimuthal plane, that is the ($\varphi = 0$) plane of the laboratory frame. The normalized DSCSs are shown in figure 2 for prolate spheroidal scatterers of axial ratio $a/b = 2$, and for two size parameters $ka = 10$ and 20 . The symmetry axis of the particle is along the Z axis. In figure 3(a) we consider a spheroid placed at the centre of the Gaussian beam with a more general orientation $\alpha = \beta = 45^\circ$. The curves for a scatterer with the same orientation but placed at $x_0 = y_0 = z_0 = 20\mu\text{m}$ in a Gaussian beam with $w_0 = 50\mu\text{m}$ are depicted in figure 3(b). Figures 4(a) and (b) show the normalized DSCSs for prolate scatterers of axial ratio $a/b = 5$ and 6 respectively, and for two size parameters $ka = 5$ and 6 . The results given in figures 2–4 clearly demonstrate that no significant differences exist between the scattering diagrams, and that the



(a)

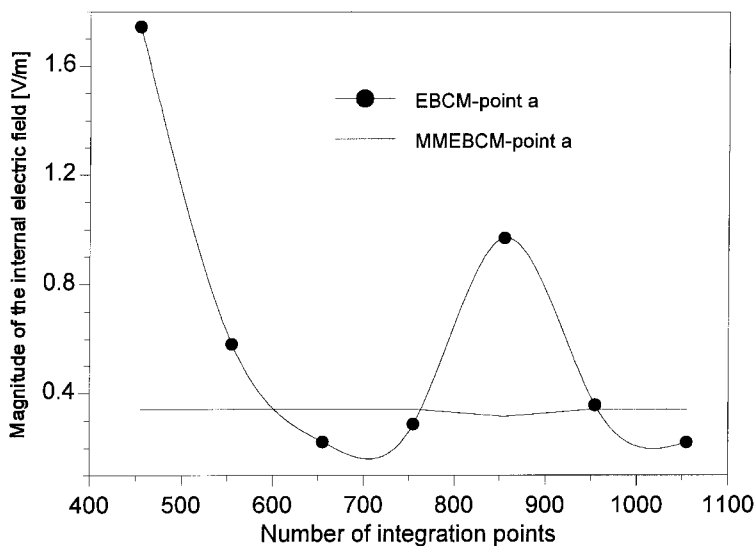


(b)

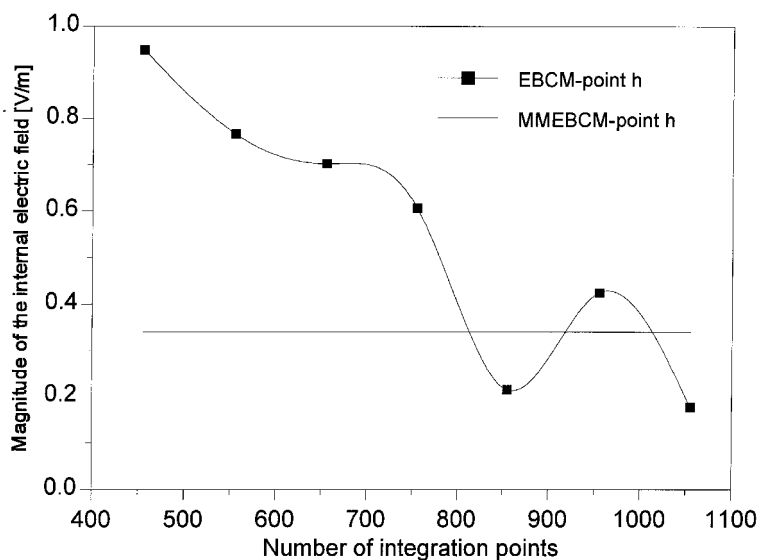
Figure 6. Magnitude of the internal field as function of the integration points for a spheroidal particle with $M = 2.236$, $a/b = 7$, $ka = 1.35$ at the points (a) a and (b) h.

MMEBCM does indeed agree quite well with the cases that could be handled by the standard formulation of the EBCM.

The objective of our final validity test is to demonstrate the applicability of the MMEBCM in the context of evaluating the interior fields induced along the symmetry axis of prolate spheroids. Even though the application of the standard formulation of EBCM has been widely found to be successful in treating problems



(a)



(b)

Figure 7. Magnitude of the internal field as function of the integration points for a spheroidal particle with $M = 2\,236$, $a/b = 10$, $ka = 1.35$ at the points (a) a and (b) h.

that involve the far-field scattering characteristics, a major limitation lies in the use of EBCM in modelling the internal fields induced inside highly elongated dielectric spheroids at frequencies at and beyond the resonance frequency range. Problems occur at points lying outside the maximum inscribed sphere, especially at the far ends of the dielectric object. We have considered a lossless dielectric spheroid with a refractive index $M = 2\,236$, which has the first resonance

Table 2. Comparison of the magnitude of the internal electric-field distribution at selected equidistant points along the symmetry axis with the IEBCM, VIEF, GMT and MMEBCM for a spheroidal particle with $a/b = 15$, $\lambda = 10 \mu\text{m}$, $a = 0.3 \mu\text{m}$ and $\epsilon_i = 3 + 1j$.

Location of field points	Internal electric field (V m^{-1})			
	IEBCM	VIEF	GMT	MMEBCM, forms (B) and (C)
a	0.483	0.473	0.4765	0.4865
b	0.487	0.487	0.4836	0.4867
c	0.489	0.488	0.4866	0.4868
d	0.488	0.489	0.4876	0.4869
e	0.489	0.492	0.4878	0.4870
f	0.488	0.487	0.4870	0.4871
g	0.490	0.484	0.4849	0.4871
h	0.488	0.473	0.4791	0.4872

frequency at $ka = 1.35$. The electric field intensities are computed at eight points equally spaced along the major axis of the spheroid for a unitary incident electric-field vector that is polarized in the X direction, as illustrated in Figure 5. The results in table 1 show that at an aspect ratio of $a/b = 4$ the MMEBCM and the EBCM agree perfectly, but, as the particle eccentricity increases, the convergence of the internal field at the far ends begins to deteriorate significantly. The oscillations of the magnitude of the internal field with the number of integration points for $a/b = 7$ and $a/b = 10$ spheroids are shown in Figures 6 and 7 respectively. These oscillations question the stability of the standard EBCM solution. In contrast, the values of the internal fields obtained by the MMEBCM are constant over the entire analysis domain. Numerical experiments with the MMEBCM have shown rapid convergence of the internal fields, which is apparent from the results given in table 2 for an $a/b = 15$ spheroid, where good agreement has been achieved with the results obtained from the GMT, the volume integral-equation formulation VIEF and the IEBCM, listed in [23].

4. Conclusions

A general formulation of the EBCM was obtained by using arbitrary complete system functions on the particle surface. By approximating the surface currents in the mean-square norm by normal multipole expansions with different origins or by the lowest-order multipoles located at the z axis of the particle, we derived various formulations of the EBCM. These EBCM formulations based on multiple-multipole expansions improve the stability and accuracy of the regular EBCM for highly elongated particles, because the boundary can be covered more efficiently by multiple multipoles.

The general case of Gaussian beam incidence was also considered, where the beam shape coefficients are computed by using the generalized localized approximation. Numerical results concerning the comparison of the axial distribution of the induced internal fields illustrate the adequacy of the EBCM formulations based on multiple-multipole expansions to calculate the scattering by spheroids with large aspect ratio.

Acknowledgments

The authors are grateful to the Deutsche Forschungsgemeinschaft for providing financial support for this work.

References

- [1] WATERMAN, P. C., 1969, *J. Acoust. Soc. Am.*, **45**, 1417.
- [2] WATERMAN, P. C., 1971, *Phys. Rev. D*, **3**, 825.
- [3] LAKHTAKIA, A., VARADAN, V. K., and VARADAN, V. V., 1984, *Appl. Optics*, **23**, 3502.
- [4] BATES, R. H. T., and WALL, D. J. N., 1977, *Phil. Trans. R. Soc. A*, **287**, 45.
- [5] HACKMAN, R. H., 1984, *J. Acoust. Soc. Am.*, **75**, 35.
- [6] BOSTRÖM, A., 1984, *J. Acoust. Soc. Am.*, **76**, 588.
- [7] HAFNER, C., 1990, *The Generalized Multipole Technique for Computational Electromagnetics* (Norwood, Massachusetts: Artech House Books).
- [8] LUDWIG, A. C., 1991, *Comput. Phys. Commun.*, **68**, 306.
- [9] EREMIN, J. A., and SVESHNIKOV, A. G., 1992, *The Discrete Sources Method in Electromagnetic Scattering Problems* (Moscow State University Publishing House) (in Russian).
- [10] LEVIATAN, Y., BOAG, A., and BOAG, A., 1991, *Comput. Phys. Commun.*, **68**, 331.
- [11] EREMIN, J. A., ORLOV, N. V., and ROZENBERG, V. I., 1994, *Comput. Phys. Commun.*, **79**, 201.
- [12] ISKANDER, M. F., LAKHTAKIA, A., and DURNEY, C. H., 1983, *IEEE Trans. Antennas Propag.*, **31**, 317.
- [13] ISKANDER, M. F., and LAKHTAKIA, A., 1984, *Appl. Optics*, **23**, 948.
- [14] WATERMAN, P. C., 1980, *Acoustic, Electromagnetic and Elastic Wave Scattering*, edited by V. K. Varadan and V. V. Varadan (Oxford: Pergamon), pp. 61–78.
- [15] HARRINGTON, R. F., 1968, *Field Computation by Moment Method* (London: Macmillan).
- [16] HIZAL, A., 1980, *Acoustic, Electromagnetic and Elastic Wave Scattering*, edited by V. K. Varadan and V. V. Varadan (Oxford: Pergamon), pp. 169–190.
- [17] MÜLLER, C., 1976, *Inst. Naz. Alta Math. Sympos. Math.*, **18**, 353.
- [18] AYDIN, K., and HIZAL, A., 1986, *J. math. Anal. Appl.*, **117**, 428.
- [19] ALBADWAIHY, K. A., and YEN, L. J., 1975, *IEEE Trans Antennas Propag.*, **23**, 546.
- [20] KERSTEN, H., 1985, *Math. Meth. appl. Sci.*, **7**, 40.
- [21] BARTON, J. P., ALEXANDER, D. R., and SCHAUB, S. A., 1988, *J. appl. Phys.*, **64**, 1632.
- [22] DOICU, A., and WRIEDT, T., 1997, *Appl. Optics* (submitted).
- [23] AL-RIZZO, H. M., and TRANQUILLA, J. M., 1996, *Appl. Optics.*, **34**, 3502.

